











## Research Article

# Protective Effects of Aqueous Extracts of the Herb of *Paederia scandens* (Lour.) Merr. against HCl/EtOH-Induced Gastric Ulcer in Rats: Involvement and Inhibitors' Identification of NF- $\kappa$ B Signaling

Qingxia Li <sup>1,2</sup>, Hui Guo <sup>1,2</sup>, Man Gong <sup>1,2</sup>, Yang Zhang <sup>1,2</sup>, Lianhe Yang <sup>1,2</sup>,  
Jing Wang <sup>1,2</sup>, Pei Wang <sup>1,2</sup>, Zhimin Wang <sup>1,2,3</sup>, Erping Xu <sup>1,2</sup> and Liping Dai <sup>1,2</sup>

<sup>1</sup>Henan University of Chinese Medicine, Henan, Zhengzhou 450046, China

<sup>2</sup>Engineering Technology Research Center for Comprehensive Development and Utilization of Authentic Medicinal Materials from Henan, Henan, Zhengzhou 450046, China

<sup>3</sup>Institute of Chinese Materia Medica, China Academy of Chinese Medical Sciences, Beijing 100700, China

Correspondence should be addressed to Erping Xu; [xuerping@sina.com](mailto:xuerping@sina.com) and Liping Dai; [liping\\_dai@hactcm.edu.cn](mailto:liping_dai@hactcm.edu.cn)

Received 18 February 2023; Revised 6 May 2023; Accepted 14 June 2023; Published 4 July 2023

Academic Editor: Kai Wang

Copyright © 2023 Qingxia Li et al. This is an open access article distributed under the Creative Commons Attribution License, which permits unrestricted use, distribution, and reproduction in any medium, provided the original work is properly cited.

*Paederia scandens* (Lour.) Merr. (*P. scandens*), as an edible and medicinal herb, is commonly used for treating gastric ulcer in China; however, its mechanistic and effective substances' studies remain limited. This study aimed to investigate the antigastric ulcer effects of aqueous extracts of *P. scandens* (PS-AE) and explore the involvement of NF- $\kappa$ B signaling in this effect. In addition, the study aimed to identify the effective substances by exploring NF- $\kappa$ B inhibitors. The main components of PS-AE were identified using an UPLC-MS method. HCl/EtOH-induced acute gastric ulcer in rats, and LPS-stimulated RAW264.7 cells were used to determine the antigastric ulcer effects of PS-AE *in vivo* and *in vitro*, respectively. Histopathological changes of the ulcer tissues were observed using staining methods of HE and PAS; secretions of inflammatory cytokines and oxidative stress indexes were measured using biochemical test kits; protein levels of NF- $\kappa$ B signaling pathway-related molecules were measured using Western Blot. NF- $\kappa$ B inhibitors' identification in *P. scandens* was performed by developing HipHop pharmacophore model, and the results were further validated by molecular docking. *In vivo*, PS-AE significantly attenuated gastric ulcer in rats; reduced inflammation by adjusting the inflammatory cytokines TNF- $\alpha$ , IL-1 $\beta$ , and IL-6 levels; and induced oxidative stress can be alleviated via adjusting the levels of SOD, MDA, and GSH-Px. In addition, PS-AE may play an anti-inflammatory role mainly through NF- $\kappa$ B signaling pathway. Following pharmacophore modeling and molecular docking, 13 potential inhibitors targeting NF- $\kappa$ B were identified. In addition, *in vitro*, PS-AE and paederoside could significantly inhibit the activation of NF- $\kappa$ B p65 and the productions of downstream cytokines including NO, TNF- $\alpha$ , and IL-6. PS-AE protective effects on gastric ulcer damage induced by HCl/EtOH in rats, which is probably associated with its antioxidant effect and the inhibitory effects on levels of inflammatory mediators regulated by NF- $\kappa$ B signaling pathway. 13 potential NF- $\kappa$ B-targeting inhibitors are probably effective substances contributing to the herb's pharmacological effect. In practical application, *Paederia scandens*, a traditional food and medicinal plant, possessed diversified chemical components and multiple pharmacological activities (anti-inflammatory, bacteriostasis, and antioxidative.). In China, *P. scandens* has been used as a traditional medicine to treat gastritis for hundreds of years, and it may be a potentially effective dietary product to improve gastric ulcer. This study shows that *P. scandens* exerts protective effects on gastric ulcer damage induced by HCl/EtOH in rats, which is probably associated with its antioxidant effect and the inhibitory effects on levels of inflammatory mediators regulated by NF- $\kappa$ B signaling pathway, which provides pharmacological justifications for the functional food use of *P. scandens* for treating gastric disease.

## 1. Introduction

Gastric ulcer, one of the most constant digestive disorders with an increasing incidence and prevalence, is affecting millions of people yearly [1, 2]. Various stimulus including alcohol and nonsteroidal anti-inflammatory medications can cause increasing incidences of gastric ulcer [3]; the imbalance between these stimulating factors and gastric mucosal protective factors (mucin and prostaglandins) leads to gastric mucosal lesions. The commonly used antiulcer therapies in clinic include antiacid drugs and H<sub>2</sub> receptor inhibitors, but these therapies are always accompanied with adverse effects such as low healing rates and high recidivism rates [4, 5]. Accordingly, it is urgently needed to explore an effective and safe alternative therapy for treating gastric ulcer. Numerous studies have indicated that inflammatory response has an important role in the pathogenesis of gastric ulcer [6]. The development of gastric ulcer is accompanied by a significant release of inflammatory factors that can lead to activation of nuclear factor- $\kappa$ B (NF- $\kappa$ B) and the translocation of NF- $\kappa$ B into the nucleus. The entry of NF- $\kappa$ B into the nucleus triggers the transcription of various inflammatory mediators (tumor necrosis factor- $\alpha$  (TNF- $\alpha$ ), interleukin-1 $\beta$  (IL-1 $\beta$ ), and interleukin-6 (IL-6)), which trigger local or systemic inflammation and cause cellular or organ dysfunction [7, 8, 9]. Therefore, inhibiting inflammatory response is an effective method to treat gastric ulcer. Traditional Chinese medicine has obvious advantages in treating gastric inflammatory response [10, 11].

*Paederia scandens* (Lour.) Merr., “Jishiteng” in Chinese, recorded in Chinese Pharmacopoeia (1977 Edition) [12], has been used as a traditional medicine to treat gastritis for hundreds of years. Various ingredients have been reported to occur in *P. scandens*, including flavonoids and iridoids [13, 14]. Modern pharmacological studies have revealed that *P. scandens* have anti-inflammatory and antioxidative activities [15, 16] and has been used to treat gastric ulcer, rheumatoid arthritis, and diarrhea [15, 17, 18]. However, its antagastric ulcer mechanistic and effective substances studies have not been fully elucidated.

In this work, we investigated the protective effects of *P. scandens* on HCl/EtOH-induced gastric ulcer in rats and explored the involvement of NF- $\kappa$ B signaling in the effects; furthermore, we explored its effective substances by using pharmacophore modeling and molecular docking, which provides pharmacological justifications for the functional food use of *P. scandens* for treating gastric disease.

## 2. Materials and Methods

**2.1. Materials.** *Paederia scandens* (Lour.) Merr. was purchased from the Bozhou, Anhui Province (LOT: 20200627). The samples were identified by Professor Dai Liping (Henan University of Chinese Medicine, China), and voucher specimens are housed at the Henan University of Chinese Medicine Herbarium. The following reagents and kits were used in the study: Phosphate-buffered saline (PBS), and fetal bovine serum (FBS), Dulbecco's modified Eagle's medium (DMEM) (Biological Industries, Kibbutz, Israel); superoxide

dismutase (SOD), malondialdehyde (MDA) and glutathione peroxidase (GSH-Px) test kits (Nanjing Jiancheng Bio-engineering Institute, Nanjing, China); Rat TNF- $\alpha$ , Rat IL-1 $\beta$ , and Rat IL-6 (MULTI SCIENCES (LIANKE) BIOTECH, Co., Ltd., Hangzhou, China); Mouse TNF- $\alpha$  and Mouse IL-6 (Wuhan Elite Biotechnology Co., Wuhan, China); lipopolysaccharide (LPS), 3-(4, 5-dimethylthiazol-2-yl)-2,5-diphenyltetrazolium bromide (MTT), Griess reagent, BCA assay Kit, and enhanced chemiluminescence (ECL) detection kit (Beijing Solarbio Ltd., Beijing, China); and paederoside, paederosidic acid, rutin, quercetin, linarin, and kaempferol (Chengdu PureChem-Standard Co., Ltd., Chengdu, China); antibodies against inhibitor of kappa B kinase- $\alpha$  (IKK $\alpha$ ), p-IKK $\alpha$ , inhibitor of NF- $\kappa$ B- $\alpha$  (I $\kappa$ B $\alpha$ ), p-I $\kappa$ B $\alpha$ , NF- $\kappa$ B p65, p-P65, and cyclooxygenase-2 (COX-2) (Cell Signaling Technology, Beverly, Massachusetts, USA).

**2.2. Preparation of Extract.** PS-AE was extracted as described in [13]. Specific operations are as follows: *P. scandens* (1.0 kg) was extracted twice with 10 L water (2 h each time) under reflux condition. After filtering the extract, the filtrate was collected and concentrated to 200 mL by rotary evaporation at 50°C under reduced pressure. Then, the concentrate was lyophilized to obtain powders; the yield of PS-AE was 12.65%.

**2.3. Chemical Analyses of PS-AE.** UPLC-Orbitrap-Exploris-120-MS determination was achieved on a Hypersil GOLD VANQUISH C18 (2.1 mm  $\times$  100 mm, 1.9  $\mu$ m) column. The mobile phase consisted of acetonitrile (A) and 0.1% aqueous formic acid (B) with a flow rate of 0.3 mL/min. The gradient elution condition was set as follows: 0 min, 5% A; 0–3 min, 5–17% A; 3–20 min, 17–20% A; and 20–25 min, 20–90% A. The injection volume was 1  $\mu$ L and the column temperature was maintained at 25°C.

MS data were acquired in fast chromatography MS<sup>2</sup> mode; the mass spectrometer parameters were set as follows [19]: the ESI was used in negative ion mode (ESI<sup>-</sup>) and in positive ion mode (ESI<sup>+</sup>). The following settings were used: the spray voltage was 2.5 kV(–) and 3.5 kV(+), the UHPLC-MS/MS mode was applied with an Orbitrap resolution of 12,000 for full-MS and 15,000 for dd-MS<sup>2</sup>, the isolation window ( $m/z$ ) was 2, the RF Lens% was 70, the sheath gas pressure was 45 Arb, the auxiliary gas pressure was 15 Arb, the sweep gas pressure was 0 Arb, the capillary temperature was 320°C, vaporizer temperature was 350°C, the scanning range was  $m/z$  80–800, and the stepped normalized collision energies (NCE) were 15, 30, and 45 eV.

**2.4. Screening for Potential NF- $\kappa$ B Inhibitors in *P. scandens* Using Pharmacophore Modeling.** This study used the common feature pharmacophore generation module in Discovery Studio software to construct a small molecule ligand-based model of the HipHop pharmacophore. 6 compounds with anti-NF- $\kappa$ B activity from references are selected as the training set and used to generate HipHop pharmacophore model. From this approach, 10 pharmacophore models were

successfully generated. Then, except for some compounds with no activity or unclear activity, 30 compounds with anti-NF- $\kappa$ B activity from references are selected as the testing set. The training set was used to train the NF- $\kappa$ B pharmacophore model, while the test set was used to evaluate its predictive performance. 10 pharmacophore models were then evaluated using the ligand profiler module in Discovery Studio to select the model with the best predictive power. A total of 99 components of *P. scandens* were collected from the TCMSP (<https://tcmisp-e.com/>) database. Based on this preprocessing, the anti-NF- $\kappa$ B activity of 99 compounds in *P. scandens* was predicted and other parameters were set as default. The structures of both training set and test set compounds are provided in Supplementary Materials (the training set is marked by \*).

**2.5. Molecular Docking Studies.** A molecular docking study of small molecule compounds predicted (pharmacophore model) using the CDocker module in Discovery Studio software. The 3D structure of the compound built by ChemOffice software was saved in \*.mol2 format, and its energy was minimized. The 3D structure of the target protein was downloaded from the PDB data (<https://www.rcsb.org/>), and Discovery Studio 2020 software was used to perform operations such as water removal and hydrogenation of the protein and generate an effective single 3D conformation by minimizing the energy.

**2.6. Experimental Animals.** Male Wistar rats (3–8 weeks old with  $180 \pm 20$  g body weight) purchased from Jinan Pengyue Experimental Animal Breeding Co., Ltd. (SYXK (Lu) 20190003) were used to study the protective effects of PS-AE on HCl/EtOH-induced gastric ulcer in rats. The experimental unit used license number SYXK (Yu) 2020–0004, and all animals were kept under environmentally controlled conditions ( $22 \pm 1^\circ\text{C}$  and  $50 \pm 10\%$  relative humidity) with a 12 h light/dark cycle and were allowed to eat, and drink, at will during the experimental period. All experimental procedures including the rat model adopted in this study conformed to the Basel Declaration and the ethical guidelines of the International Council for Laboratory Animal Science (ICLAS). The experimental protocol was approved by the Animal Ethics Committee of Henan University of Traditional Chinese Medicine, ethics number: DWLL202009059. The rats were allowed to acclimatize to the laboratory environment for one week before the experiment.

**2.7. Animal Modeling, Grouping, and Drug Administration.** 40 rats were randomly divided into 5 groups of 8 rats each. Gastric ulcer was induced in rats by HCl/EtOH (take an appropriate amount of HCl and dissolve it in 60 : 40 ethanol : water (v : v) solution to get a concentration of 150 mmol/L HCl/EtOH.) as described previously [20]. Rats in the administration group received PS-AE (50 and 100 mg/kg) or ranitidine (35 mg/kg) twice a day for three days, whereas the control group and model group received vehicle (1% CMC-

Na) twice a day for three days, the experimental doses of PS-AE and ranitidine were determined according to references and the result of pre-experiments [20]. The animals were fasted overnight with free access to water before the experiment, 30 minutes after the last PS-AE treatment; 2 mL of HCl/EtOH was administered via oral gavage. 1 h after the HCl/EtOH treatment, the rats were anesthetized, the stomachs were removed and immediately washed in ice-cold saline, images were recorded with a digital camera, and the area ( $\text{mm}^2$ ) of each mucosal erosion lesion was measured using ImageJ software.

**2.8. Gastric Histopathology and Mucosal Glycoprotein Assay in Rats with Gastric Ulcer.** Hematoxylin-eosin (HE) staining was used for histopathological observation of the gastric mucosa, and periodic acid-Schiff (PAS) staining was used to assess gastric mucosal glycoprotein. Gastric tissues from each group were fixed in 4% paraformaldehyde solution for 24 h, dehydrated through an ethanol (75–100%), and then cleared with xylene. The gastric samples were embedded in paraffin, selected for typical ulcerated areas, cut into  $5.0 \mu\text{m}$ , and stained using HE and PAS, and then placed under a light microscope for observation.

**2.9. Determination of SOD, MDA, GSH-Px, TNF- $\alpha$ , IL-1 $\beta$ , and IL-6 in Gastric Tissues.** The stomach tissue was rinsed with cold PBS and the typical ulcerated area was homogenized in phosphate buffer (pH 7.4); the homogenate was centrifuged at 10,000 g for 15 min at  $4^\circ\text{C}$ . The levels of SOD, MDA, GSH-Px, TNF- $\alpha$ , IL-1 $\beta$ , and IL-6 in the supernatant were detected by biochemical detection kits.

**2.10. Cell Culture.** The RAW264.7 macrophage cell line was purchased from Procell Life Science and Technology Co., Ltd. RAW264.7 cells were cultured in high-glucose DMEM supplemented with 10% FBS, 100 U/mL penicillin, and 100 U/mL streptomycin. Then, they were placed in a  $37^\circ\text{C}$  thermostat incubator and in a humid atmosphere with 5%  $\text{CO}_2$ .

**2.11. Cell Viability Assay.** RAW264.7 cells ( $1 \times 10^5$  cells/mL), seeded in 96-well plates and cultured overnight for adhere, were then treated with various concentrations of PS-AE (0, 6.25, 12.5, 25, 50, and 100  $\mu\text{g}/\text{mL}$ ) and paederoside (0, 6.25, 12.5, 25, 50, and 100  $\mu\text{M}$ ) in the presence or absence of LPS (1  $\mu\text{g}/\text{mL}$ ) for 24 h. Thereafter, cell viability was examined using the conventional MTT assay as stated before [21].

**2.12. Measurements of NO, TNF- $\alpha$ , and IL-6 Production.** RAW264.7 cells ( $2 \times 10^6$  cells/mL), seeded in 6-well plates and cultured overnight for adhere, were then treated with various concentrations of PS-AE (0, 12.5, and 25  $\mu\text{g}/\text{mL}$ ) and paederoside (0, 12.5, and 25  $\mu\text{M}$ ) in the presence of LPS (1  $\mu\text{g}/\text{mL}$ ) for 24 h. Supernatants were collected, and NO content was then measured by the Griess reagents, and TNF- $\alpha$  and IL-6 levels were then measured by the ELISA kits.

**2.13. Western Blot Analysis.** The proteins in tissues and cells were extracted. Protein concentrations were determined using the BCA assay kit. Equal amount of protein (40  $\mu$ g each) was resolved by electrophoresis 10% SDS-polyacrylamide gel electrophoresis (SDS-PAGE) gels and transferred to Immobilon-NC transfer membrane. The membrane was blocked with 5% nonfat dry milk with 0.5% Tween-20 (TBST) for 1 h; then, the membrane was incubated overnight at 4°C with the primary antibodies, followed by incubation with appropriate secondary antibodies for 1 h at room temperature. The primary antibody dilutions were prepared as follows: anti-IKK $\alpha$  (1:1000), anti-p-IKK $\alpha$  (1:1000), anti-I $\kappa$ B $\alpha$  (1:1000), anti-p-I $\kappa$ B $\alpha$  (1:1000), anti-P65 (1:1000), anti-p-P65 (1:1000), anti-COX-2 (1:1000), and anti- $\beta$ -actin (as internal reference); goat anti-rabbit IgG (1:10000) conjugated was used as the secondary antibody. The bands were visualized using the ECL detection kit.

**2.14. Statistical Analysis.** Statistical analysis was performed using GraphPad Prism 8.0.1 (GraphPad Software, CA, USA). Results are expressed as mean  $\pm$  standard deviation (SD); multiple group comparisons were performed using one-way ANOVA, followed by the Tukey multiple-comparison test. Significance was set at  $p < 0.05$  and  $p < 0.01$ .

### 3. Results

**3.1. Identification of the Constituents of PS-AE.** A total of 24 compounds were tentatively identified based on accurate mass, retention times, major fragment ions, online databases and published articles (Figure 1 and Table 1). Among these, compounds 2, 4, 9, 11, 16, and 18 were found to be consistent with the retention times, secondary fragmentation, and other information of the standard pederisic acid, rutin, quercetin, pederiside, linarin, and kaempferol.

**3.2. PS-AE Significantly Attenuated the HCl/EtOH-Induced Gastric Ulcer in Rats.** As shown in Figure 2(c), the lesion was barely visible in the control gastric tissue. Compared to the control group, the HCl/EtOH-induced model group showed obviously severe lesions and significantly larger ulcerated areas ( $50.35 \pm 12.41$  mm<sup>2</sup>). PS-AE showed a significant reduction in the lesion site and ulcer area compared to the model group (50 mg/kg:  $8.801 \pm 4.22$  mm<sup>2</sup>, 79.14% ulcer healing rate; 100 mg/kg:  $2.22 \pm 2.66$  mm<sup>2</sup>, 95.47% ulcer healing rate) in a dose-dependent manner. Statistical analyses of the ulcer area are shown in Figure 2(b). HE staining results (Figure 2(d)) showed that the gastric mucosa in the control group was intact without any visible bleeding or ulceration. Among the model group, the stomachs presented with severe mucosal ulcers, bleeding, edema, and inflammatory cell infiltration. The PS-AE treatment attenuated this damage in a dose-dependent manner. In fact, gastric mucosal glycoprotein form a viscoelastic mucus gel layer that protects and lubricates the lower epithelial layer of the gastric tissue and therefore plays a vital defensive role in preventing gastric ulcer [22]. PAS staining results (Figure 2(d)) showed that the staining intensity of gastric

mucosal glycoprotein was potent in the control group, where the intensity of PAS staining in the model group was obviously weakened, indicating the injuries of mucosal glycoprotein. Compared to the model group, PS-AE treatment markedly reversed the weakened staining intensity, indicating the protective effects on glycoprotein in the gastric mucosa. To sum up, PS-AE significantly attenuated the HCl/EtOH-induced gastric ulcer in rats.

**3.3. PS-AE via NF- $\kappa$ B Pathway Plays a Therapeutic Role and Implicates Inflammation and Oxidative Stress.** As shown in Figure 3(a), the levels of TNF- $\alpha$ , IL-6, and IL-1 $\beta$  in the model group were significantly higher than those in the control group. Compared to the model group, PS-AE significantly inhibited the increase in TNF- $\alpha$ , IL-1 $\beta$ , and IL-6 levels. As shown in Figure 3(b), versus control group, the MDA levels in the model group were significantly increased, but the SOD and GSH-Px levels were decreased. Compared to the model group, PS-AE significantly inhibited the increase in MDA levels but the decrease in SOD and GSH-Px levels. As shown in Figure 3(c), versus control group, the phosphorylated protein levels of IKK $\alpha$ , I $\kappa$ B $\alpha$ , and P65 and the protein level of COX-2 in the gastric tissue of the model group were abnormally up-regulated. PS-AE significantly decreased the HCl/EtOH-induced upregulation on phosphorylation protein levels of IKK $\alpha$ , I $\kappa$ B $\alpha$ , and P65 and protein levels of COX-2 in gastric tissues.

**3.4. Screening of 13 Potential Inhibitors of NF- $\kappa$ B in *P. scandens* Using Pharmacophore Modeling and Molecular Docking.** In this study, pharmacophore models were constructed based on 6 training sets of molecules. A total of 395 pharmacophore elements, including 217 hydrogen bond acceptors, 159 hydrogen bond donors, 15 hydrophobic groups, 2 positive charge centers, and 2 aromatic ring centers, were extracted by feature mapping, and the results are shown in Figure 4(a). These characteristic elements were selected, and a total of 10 pharmacophore models were generated using the HipHop method, the resulting parameters of which are shown in Table 2. The scores refer to the match between the molecules in the training set and the pharmacophore model, and it can be seen that the 10 pharmacophores generated all scored over 60, demonstrating that the molecules selected for the test set share common features, with pharmacophore 01 scoring 74.808 and the rest of the pharmacophores scoring relatively close to each other. Combining the results of the pharmacophore thermogram, where the warm shades represent a high response to ligands and the cool shades represent a low response to ligands, it can be seen that pharmacophore 01 is more responsive to the active compounds in the test set and less responsive to the inactive compounds (Figure 4(b)), so pharmacophore 01 was chosen as the subject for subsequent studies. From the results, it can be observed that the preferred pharmacophore 01 consists mainly of 4 hydrogen-bonded receptors, 1 hydrophobic center, and 2 hydrogen bond donors (Figure 4(a)).

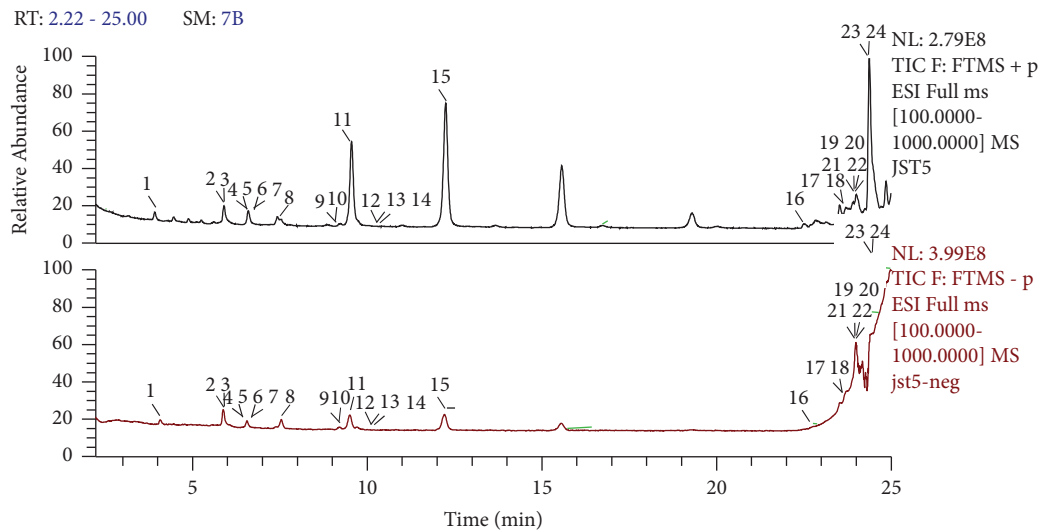


FIGURE 1: UPLC-MS chromatogram of the PS-AE in total ion flow diagram. Peak numbering follows the one stated in Table 1.

A virtual screening of the potential NF- $\kappa$ B inhibitors in *P. scandens* using the validated preferred pharmacophore model resulted in a total of 14 potential NF- $\kappa$ B inhibitors (Figure 4(c)), including linarin, scandoside methyl ester, asperuloside, paederoside, paederosidic acid methyl ester, kaempferol 7-O- $\beta$ -D-glucopyranoside, deacetyl asperulosidic acid methyl ester, rutin, geniposide, astragalol, quercimeritrin, quercetin, hirsutrin, and deacetyl asperulosidic acid. The fit value of the pharmacophore decreased sequentially from 3.42868 to 0.518575, the results are shown in Table 3.

The screened constituents were docked to NF- $\kappa$ B p65 (PDB ID: 5URN). Active ingredients with CDOCKER\_INTERACTION\_ENERGY  $\leq -5.0$  kJ/mol were selected as the screening basis for their anti-NF- $\kappa$ B activity effects. The results are shown in Table 3 and Figure 4(d), scandoside methyl ester, asperuloside, paederoside, paederosidic acid methyl ester, kaempferol 7-O- $\beta$ -D-glucopyranoside, deacetyl asperulosidic acid methyl ester, rutin, Geniposide, astragalol, quercimeritrin, quercetin, hirsutrin, and deacetyl asperulosidic acid showed potent binding abilities to NF- $\kappa$ B p65. Then, paederoside was selected for *in vitro* verification in this study.

**3.5. PS-AE and Paederoside Could Significantly Inhibit the Activation of NF- $\kappa$ B p65 and the Production of Inflammatory Factors in Downstream Cells.** As shown in Figure 5(b), PS-AE showed no cytotoxic effects at 12.5–50  $\mu$ g/mL (cell viability was above 90%), and the viability was slightly decreased at a high concentration (100  $\mu$ g/mL). Thus, the concentrations 12.5 and 25  $\mu$ g/mL were used in subsequent experiments. In addition, at all concentrations of 6.25–100  $\mu$ M, the cell viability of paederoside was above 90%, so 12.5 and 25  $\mu$ M were used in the subsequent experiments. As shown in Figure 5(c), PS-AE and paederoside significantly decreased the LPS-stimulated upregulation on phosphorylation protein levels of NF- $\kappa$ B p65 in RAW264.7 cells. As shown in Figure 5(d), compared with the control

group, the productions of NO, TNF- $\alpha$ , and IL-6 in the model group were significantly increased. Versus model group, PS-AE (12.5 and 25  $\mu$ g/mL) and paederoside (12.5 and 25  $\mu$ M) had dose dependently inhibited the levels of NO, TNF- $\alpha$ , and IL-6.

#### 4. Discussion

*Paederia scandens* (Lour.) Merr., as an edible and medicinal plant, can be used to treat many digestive diseases. Several historical documents have described the protective effects of *P. scandens* on gastric ulcer. However, the mechanism of action of this herb for treating gastric ulcer remains unclear. As our results indicated, PS-AE treatment significantly attenuated HCl/EtOH-induced gastric tissue damage, which was probably associated with inhibition activities of oxidative stress and pro-inflammatory mediators regulated by NF- $\kappa$ B signaling pathway.

As many studies reported, HCl/EtOH-induced gastric ulcer model has been used as a robust model resembling pathogenesis of gastritis or gastric ulcer [23, 24]. Ethanol is a noxious factor that can negatively influence gastric mucosa [25]; numerous studies have demonstrated that the pathological characteristics of gastric mucosa in alcohol-treated experimental animals are similar to those in humans consuming excessive alcohol such as abnormal gastric acidity and stomach bleeding [26]. Hydrochloric acid is a strong acid that can directly damage the gastric mucosa [20].

In this study, we prepared aqueous extracts (decoction) of *P. scandens* using the traditional decocting method for Chinese medicine. These decoctions are mixed solvents that can take on various forms, such as turbidity, suspension, gel, colloid, and solvent. The colloid and gel components can adhere to the surface layer of the gastric mucosa, which in turn can help block the erosive effects of gastric acid [27]. In addition, the decoctions are generally weakly acidic, which allows them to buffer the acidic gastric juice and achieve an acid-suppressing effect. The decoction contains nutrients like protein and polysaccharides that can provide direct

TABLE 1: Chemical constituents identified in PS-AE by using UPLC-MS<sup>2</sup>.

Peak no.	Analyst	Rt (min)	Molecular formula	Calc. MW	Error (ppm)	MS <sup>1</sup> (m/z)	MS <sup>2</sup> (m/z)
1	Asperulosidic	4.07	C <sub>18</sub> H <sub>24</sub> O <sub>12</sub>	432.1270	0.52	431.016 [M - H] <sup>-</sup>	269.0650, 251.0565, 225.0770, 207.0668, and 183.0668
2	Paederosidic acid <sup>S</sup>	5.89	C <sub>18</sub> H <sub>24</sub> O <sub>12</sub> S	464.0983	1.12	463.0909 [M - H] <sup>-</sup>	428.2374, 371.0979, 283.0290, 264.0499, 209.0457, 191.0350, 165.0558, 47.0453, and 123.0458
3	Benzoic acid	5.93	C <sub>7</sub> H <sub>6</sub> O <sub>2</sub>	122.0369	0.69	121.0297 [M - H] <sup>-</sup>	115.9207, 109.9421, 91.9315, and 77.0045
4	Rutin <sup>S</sup>	6.58	C <sub>27</sub> H <sub>30</sub> O <sub>16</sub>	610.1528	3.12	609.1469 [M - H] <sup>-</sup>	365.9859, 343.0457, 300.0279, 273.0397, and 151.0633
5	Laricresinol-4-O-glucoside	6.71	C <sub>26</sub> H <sub>34</sub> O <sub>11</sub>	522.2107	1.14	521.2059 [M - H] <sup>-</sup>	476.6039, 359.1505, 307.8777, and 89.0249
6	5,7-Dihydroxy-2-methylbenzopyran-4-one	6.78	C <sub>10</sub> H <sub>8</sub> O <sub>4</sub>	192.0416	-3.44	193.0489 [M + H] <sup>+</sup>	178.0251, 149.0226, 139.0382, 133.0272, 121.0280, and 103.0172
7	Scopoletin	6.88	C <sub>10</sub> H <sub>8</sub> O <sub>4</sub>	192.0416	-3.44	193.0483 [M + H] <sup>+</sup>	175.0476, 165.0273, and 147.0166
8	Coumarone	7.52	C <sub>8</sub> H <sub>6</sub> O	118.0414	-3.69	119.0488 [M + H] <sup>+</sup>	105.0445, 92.0572, 91.0540, and 79.0540
9	Quercetin <sup>S</sup>	9.20	C <sub>15</sub> H <sub>10</sub> O <sub>7</sub>	302.0421	-3.06	303.049 [M + H] <sup>+</sup>	285.0390, 257.0443, 229.0476, and 165.0188
10	Astragaln	9.23	C <sub>21</sub> H <sub>20</sub> O <sub>11</sub>	448.1011	3.76	447.0936 [M - H] <sup>-</sup>	300.0278, 283.0248, 255.0310, and 151.0043
11	Paederoside <sup>S</sup>	9.55	C <sub>18</sub> H <sub>22</sub> O <sub>11</sub> S	446.0877	4.12	447.0937 [M + H] <sup>+</sup>	300.0278, 283.0224, 271.0248, 255.0291, 151.0042, and 121.0293
12	Ustilaginoidin A	9.72	C <sub>28</sub> H <sub>18</sub> O <sub>10</sub>	514.0916	3.17	513.0844 [M - H] <sup>-</sup>	361.2084
13	Diatryene 3	9.74	C <sub>10</sub> H <sub>6</sub> O <sub>3</sub>	174.0312	-3.07	175.0384 [M + H] <sup>+</sup>	147.0437, 131.0482, 119.0488, 116.0702, and 91.0540
14	(3S,5S,6S)-Communiol C	10.44	C <sub>9</sub> H <sub>16</sub> O <sub>4</sub>	188.1049	0.15	189.0542 [M + H] <sup>+</sup>	161.0608 and 129.0336
15	Halstocacosanolide C	12.27	C <sub>48</sub> H <sub>78</sub> O <sub>10</sub>	814.5578	-2.04	815.5667 [M + H] <sup>+</sup>	637.9799, 567.1544, 365.2295, and 147.0263
16	Linarin <sup>S</sup>	22.42	C <sub>28</sub> H <sub>32</sub> O <sub>14</sub>	592.1786	-2.16	593.1852 [M + H] <sup>+</sup>	285.0748 and 85.0280
17	Apigenin 5-(6''-malonylglucoside)	23.68	C <sub>24</sub> H <sub>22</sub> O <sub>13</sub>	518.1058	-0.43	517.0994 [M + H] <sup>+</sup>	401.0883, 383.0761, 357.0623, 313.0720, and 225.0555
18	Kaempferol <sup>S</sup>	23.77	C <sub>15</sub> H <sub>10</sub> O <sub>6</sub>	286.0472	-0.55	287.0539 [M - H] <sup>-</sup>	287.0548, 258.0511, 183.0288, 165.0183, 153.0189, 133.0292, and 121.0281
19	Isoliquiritigenin	23.89	C <sub>15</sub> H <sub>12</sub> O <sub>4</sub>	256.0727	-3.2	257.0801 [M + H] <sup>+</sup>	162.0707, 147.0437, 137.0233, and 121.0276
20	Apigenin 7-(2''-acetyl-6''-methylglucuronide)	23.89	C <sub>24</sub> H <sub>22</sub> O <sub>12</sub>	502.1107	-0.88	501.1043 [M - H] <sup>-</sup>	399.1078, 255.0666, 193.0475, and 153.0205
21	Daphyloside	23.90	C <sub>19</sub> H <sub>26</sub> O <sub>12</sub>	446.4025	4.1	445.1147 [M - H] <sup>-</sup>	445.1147, 401.0883, 357.0987, 313.0714, 281.0048, 255.0665, 225.0559, 181.0658, and 135.0090
22	Radicinin	24.00	C <sub>12</sub> H <sub>12</sub> O <sub>5</sub>	236.0678	-3.06	237.0749 [M + H] <sup>+</sup>	204.1709, 193.0490, and 149.0229
23	Daidzein	24.10	C <sub>21</sub> H <sub>20</sub> O <sub>9</sub>	416.1113	2.51	415.1034 [M - H] <sup>-</sup>	357.0621, 313.0921, 291.0044, 271.0013, 225.0559, 181.0661, and 121.0296
24	Nobiletin	24.63	C <sub>21</sub> H <sub>22</sub> O <sub>8</sub>	402.1305	-2.38	401.0900 [M - H] <sup>-</sup>	357.0635, 313.0721, 225.0563, 181.0658, and 121.0296

Note: S means having been verified by standards.

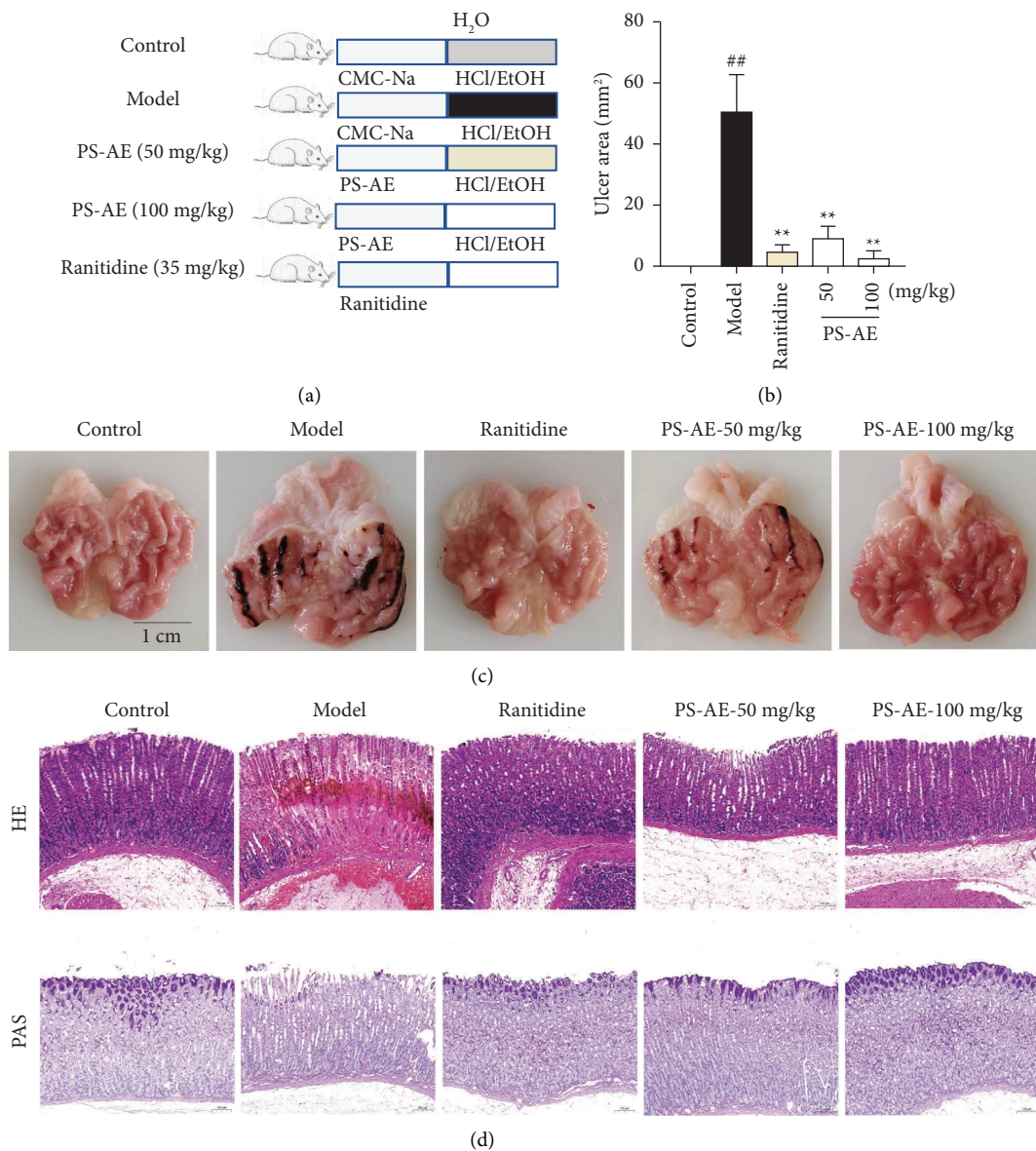


FIGURE 2: PS-AE attenuated the HCl/EtOH-induced gastric ulcer in rats: (a) experimental grouping, (b) ulcer area ( $n = 8$ ), (c) representative macroscopic images of gastric tissue damage, and (d) histopathological analysis of the stomach tissue by HE staining and mucin by PAS staining. Results are expressed as the mean  $\pm$  SD,  $**p < 0.01$  vs. model group, and  $^{##}p < 0.01$  vs. control group.

nourishment to the epithelial cells of gastric mucosa and promote metabolism [28]. In conclusion, PS-AE suspension may physically protect the gastric mucosa, but its medicinal substances still need to be explored in our further study.

In our pre-experiment, we investigated the protective effect of PS-AE at various doses (25, 50, 100, and 200 mg/kg) on HCl/EtOH-induced ulcers in rats. Results showed that PS-AE at 50 and 100 mg/kg exerted a significant protective effect on HCl/EtOH-induced gastric ulcers in rats in a dose-dependent manner. Therefore, corresponding assays at doses of 50 and 100 mg/kg in the subsequent experiments were performed, and administration of the herbal extract twice daily for three days was performed following routine pharmacological studies as literatures extensively reported [20, 29, 30]. Clinical treatment drugs for gastric ulcer include

proton pump inhibitors and H<sub>2</sub> receptor antagonists, which are effective in reducing gastric acid secretion and protecting the gastric mucosa when administered 30 minutes before a meal [22]. Therefore, our study followed this approach by modeling with HCl/EtOH 30 minutes after the last dose to evaluate the protective effect of PS-AE on gastric ulcers. The results showed that HCl/EtOH-induced severe gastric tissue damage in the model group, accompanied by a great number of visible hemorrhage spots. Compared with the model group, the ulcer area and bleeding points were significantly decreased in PS-AE-treated rats, indicating the effectiveness of PS-AE in reducing HCl/EtOH-induced gastric tissue damage.

The gastric tissue could defend against various endogenous and exogenous injuries [31]. The layer of mucus, as the

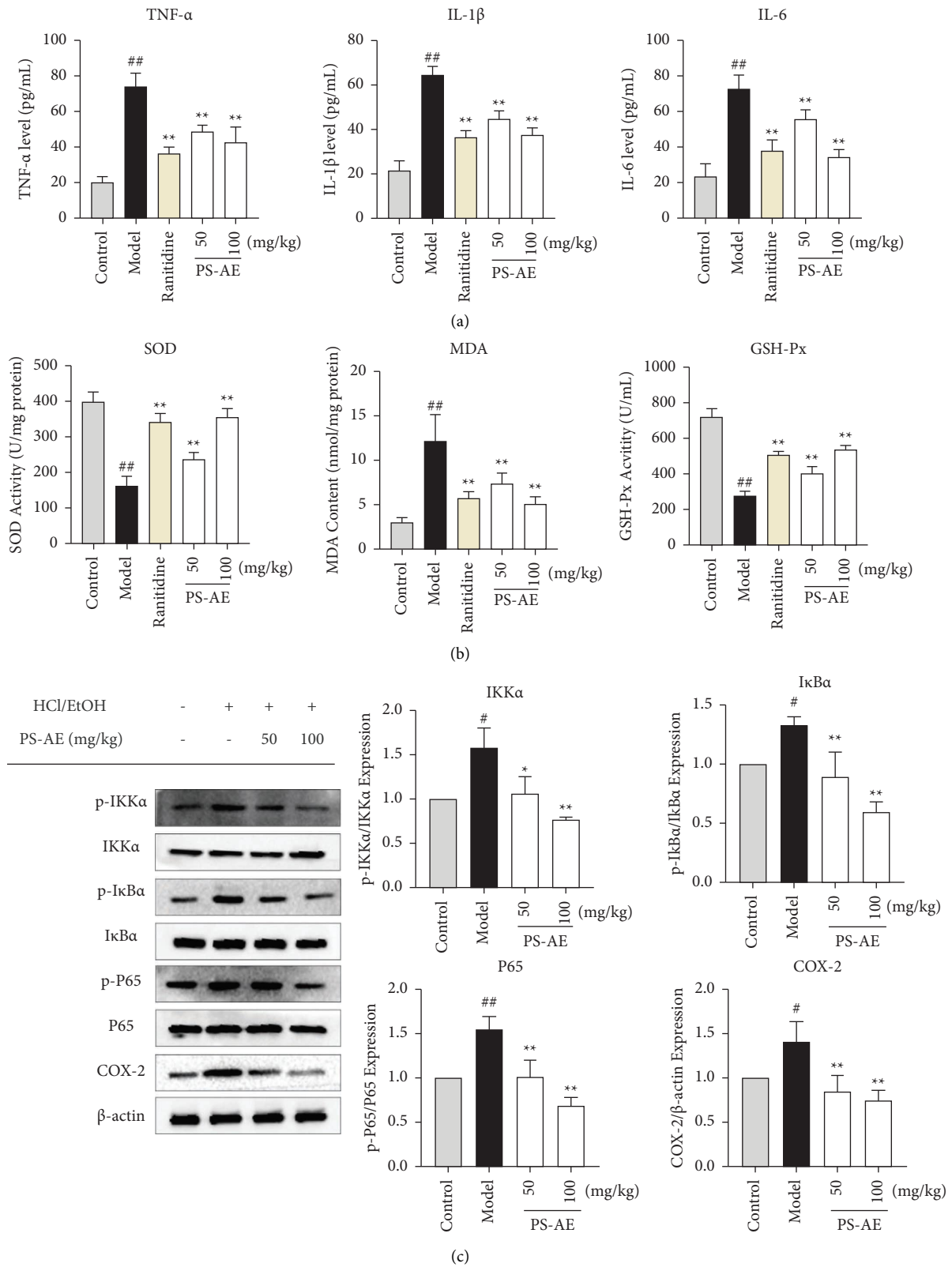


FIGURE 3: PS-AE via NF- $\kappa$ B pathway plays a therapeutic role and implicates inflammation and oxidative stress: (a) the levels of TNF- $\alpha$ , IL-1 $\beta$ , and IL-6 in gastric tissues in rats ( $n = 8$ ), (b) the levels of SOD, MDA, and GSH-Px in gastric tissues in rats ( $n = 8$ ), and (c) the expression of IKK $\alpha$ , I $\kappa$ B $\alpha$ , P65, and COX-2 in gastric tissues in rats ( $n = 3$ ). Results are expressed as the mean  $\pm$  SD, \*  $p < 0.05$ , \*\*  $p < 0.01$  vs. model group, #  $p < 0.05$ , and ##  $p < 0.01$  vs. control group.



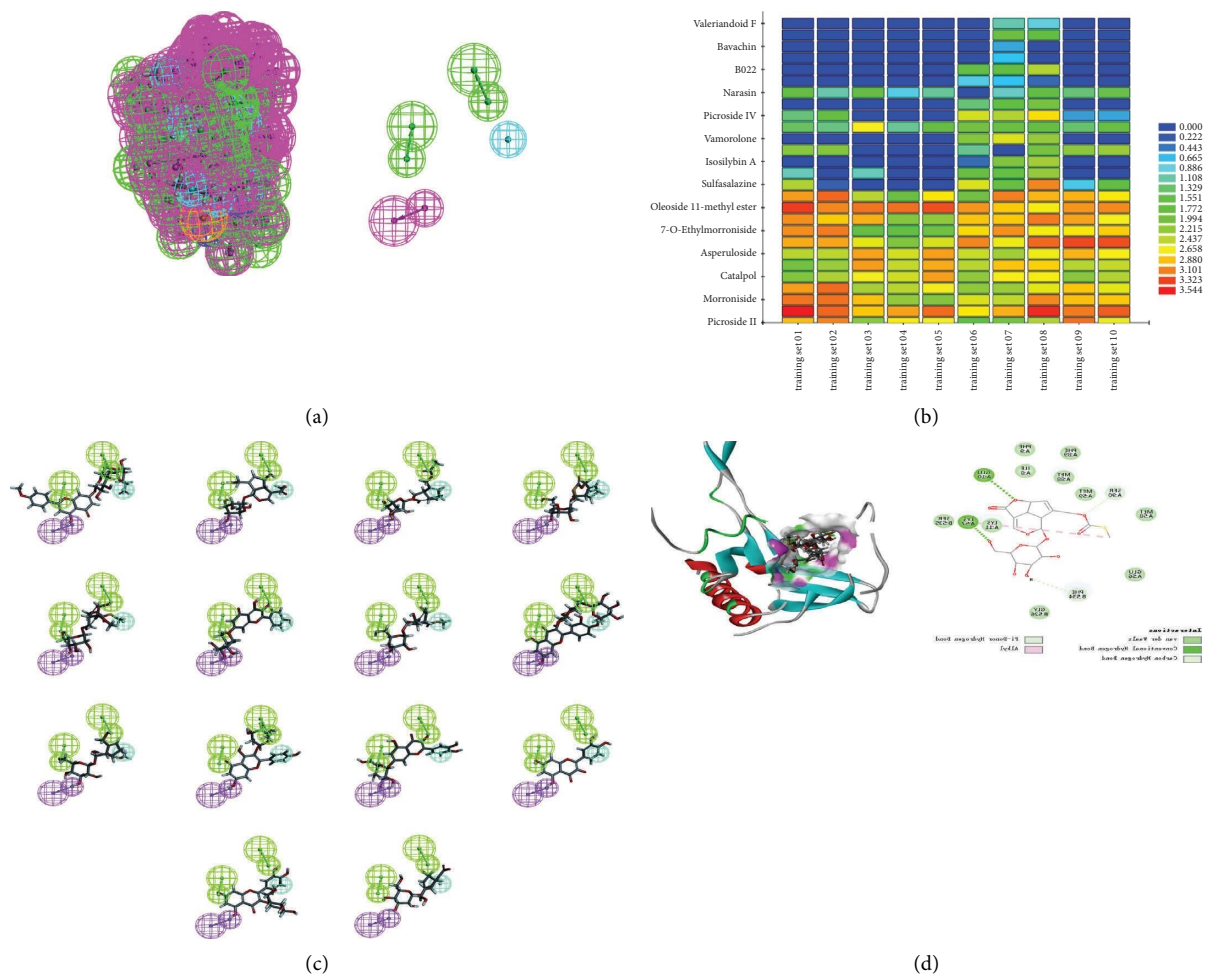


FIGURE 4: Screening of 13 potential inhibitors of NF- $\kappa$ B in *P. scandens* using pharmacophore modeling and molecular docking studies: (a) results of pharmacodynamic characteristic elements. The green sphere represents the hydrogen bond acceptor, the purple sphere represents the hydrogen bond donor, the blue sphere represents the hydrophobic group, the red sphere represents the positive charge center, and the yellow sphere represents the aromatic ring center; preferred pharmacophore model 01. It contains mainly 4 hydrogen-bonded receptors, 1 hydrophobic center, and 2 hydrogen bond donors. (b) Ligand profiler heat map. (c) The matching pattern diagram between pharmacophore model 01 and 14 potential NF- $\kappa$ B inhibitors in *P. scandens*. A–M are linarin, scandoside methyl ester, asperuloside, paederoside, paederosidic acid methyl ester, kaempferol 7-O- $\beta$ -D-glucopyranoside, deacetyl asperulosidic acid methyl ester, rutin, geniposide, astragalins, quercimeritrin, quercetin, hirsutrin, and deacetyl asperulosidic acid. (d) The interaction of NF- $\kappa$ B p65 with paederoside was studied by molecular docking, and the docking results were expressed in 3D and 2D formats.

TABLE 2: The details of ten hypotheses generated by HipHop.

Hypo	Features	Rank	Direct hit	Partial hit	Max fit
1	HDDA	74.808	111111	000000	4
2	HDDA	74.808	111111	000000	4
3	HDDA	74.289	111111	000000	4
4	HDDA	74.289	111111	000000	4
5	HDDA	74.289	111111	000000	4
6	HDAA	73.679	111111	000000	4
7	HDAA	73.679	111111	000000	4
8	HDAA	73.679	111111	000000	4
9	HDDA	73.476	111111	000000	4
10	HDDA	73.476	111111	000000	4

Note: Each row represents a pharmacophore model. The meaning of each column is as follows (using 01 as an example). Features: HDDA, this pharmacophore contains 1 hydrophobic feature, 2 hydrogen bond donors, and 1 hydrogen bonding acceptor feature. Rank: 74.808, the scoring value for this pharmacophore model is 74.808. Direct hit: 111111, the potency profile of this pharmacophore model is matched to all 6 small molecules. Partial hit: 000000, this pharmacophore model matches the 6 small molecule fractions with a number of potency profiles of 0. Max fit: 4, maximum match value is 4, i.e., all 4 potency characteristics can be matched.

TABLE 3: Pharmacophore matching and docking scores.

No.	Name	-CDOCKER interaction energy (kJ.mol <sup>-1</sup> )	Fit value
1	Linarin	—	3.42868
2	Scandoside methyl ester	42.8481	2.87856
3	Asperuloside	44.4987	2.83546
4	Paederoside	47.4163	2.78494
5	Paederosidic acid methyl ester	43.2576	2.68392
6	Kaempferol 7-O- $\beta$ -D-glucopyranoside	72.4259	2.62976
7	Deacetyl asperulosidic acid methyl ester	41.5899	2.42258
8	Rutin	55.3682	2.33174
9	Geniposide	44.4471	2.33163
10	Astragaln	57.683	2.31512
11	Quercimeritrin	59.3015	2.29535
12	Quercetin	60.8575	1.38963
13	Hirsutrin	60.4102	1.56922
14	Deacetyl asperulosidic acid	48.9971	0.518575

essential defense, protects the tissue from attacking substances such as stomach acid. As a vital defensive role in protecting against gastric ulcer, mucus glycoproteins form a viscoelastic mucus gel layer function to protect and lubricate the underlying epithelium of the gastric tissue [32]. HE staining results showed that HCl/EtOH caused edema and inflammatory cell infiltration in the gastric mucosa; these phenomena in the gastric mucosa were significantly improved after PS-AE treatment. The PAS staining results showed that HCl/EtOH caused by great deficiency of mucosal glycoprotein in gastric tissues. When treated with PS-AE, the condition of mucosal glycoproteins in gastric tissues was obviously improved, which indicated the protective effects of PS-AE on the gastric mucus layer.

It has been shown that the pathogenesis of gastric ulcer is closely associated with oxidative stress [33]. Oxidative stress is produced by a large amount of reactive oxygen species (ROS) which then causes lipid peroxidation and production of MDA [34]. SOD and GSH-Px are two vital antioxidants that can clear free radicals in the body, protecting the body from oxidative stress damage [35–37]. The results obtained in our work showed that PS-AE could protect against HCl/EtOH-induced gastric tissue damage in rats by improving oxidative stress.

NF- $\kappa$ B is the most prominent pathway regulating inflammation, and abnormal regulation of NF- $\kappa$ B may cause autoimmune diseases, chronic inflammation, and some cancers [38]. It has been shown that HCl/EtOH stimulation results in activating NF- $\kappa$ B which leads to phosphorylation of I $\kappa$ B $\alpha$  and P50/P65 heterodimer, followed by translocation to the nucleus, thus prompting cells to secrete inflammatory factors (e.g., TNF- $\alpha$ , IL-1 $\beta$ , and IL-6) and inducing an inflammatory response [39]. Elevated levels of TNF- $\alpha$  could stimulate leukocytes to secrete more IL-1 $\beta$  and IL-6, thus causing even more potent inflammatory response [40]. IL-1 $\beta$  is involved in ulcer formation [41], and elevated IL-1 $\beta$  exacerbates ulcer formation. Increased secretion of IL-6 stimulates neutrophil sites, and triggers oxidative stress, which leads to gastric mucosal damage [42]. COX-2 regulates the levels of PGE<sub>2</sub>, which enhances gastric mucosal repair [43]. The results of this study showed that PS-AE

significantly decreased the levels of pro-inflammatory mediators such as TNF- $\alpha$ , IL-6, and IL-1 $\beta$ , suggesting that the protective effects of PS-AE against HCl/EtOH-induced gastric ulcer and involvement of NF- $\kappa$ B signaling pathway in the effects.

In recent years, molecular simulation technologies such as pharmacophore model and molecular docking have been utilized for new drug research and development [44, 45]. The HipHop model is used to identify chemical features common to a range of small ligand molecules and automatically generates pharmacophore models based on the superposition of these common characteristic structures; ligand-based pharmacophore strategy has been universally used to screen small molecule-leading compounds in drug development [46]. Molecular docking is a potent method for analysing molecular interaction [47]. It was found that pro-inflammatory cytokines are secreted at the onset of gastric ulcer and play a key role in acute phase inflammation as well as in regulating the severity of gastric ulcer [22, 48, 49]. NF- $\kappa$ B is the main transcription factor that amplifies the inflammatory response such that the NF- $\kappa$ B inflammatory cascade in gastric ulcer highlights that inhibition of NF- $\kappa$ B activity plays a key role in the development of gastric ulcer [50]; [51, 52]. Pharmacophore and molecular docking results show that there are 13 compounds included the major active substances in *P. scandens* [53]; [15], including 7 iridoids and 6 flavonoids. Interestingly, paederoside, a substantial component of *P. scandens*, has a high fit value to the optimal pharmacophore model and has powerful binding abilities to NF- $\kappa$ B p65, so it was selected for *in vitro* validation in this study.

LPS-stimulated RAW264.7 macrophages are considered a canonical model for inflammatory research. Upon LPS binding to toll receptor 4 (TLR4) in immune cells, such as macrophages and neutrophils, a great amount of inflammation related factors (e.g., NO, TNF- $\alpha$ , IL-1 $\beta$ , and IL-6) was released [54]. NO, as an essential inflammatory factor, is catalysed by inducible nitric oxide synthase (iNOS), which often causes oxidative stress and cellular damage [5]. TNF- $\alpha$  could trigger an inflammatory response by promoting neutrophil infiltration [55]; TNF- $\alpha$  at high concentration

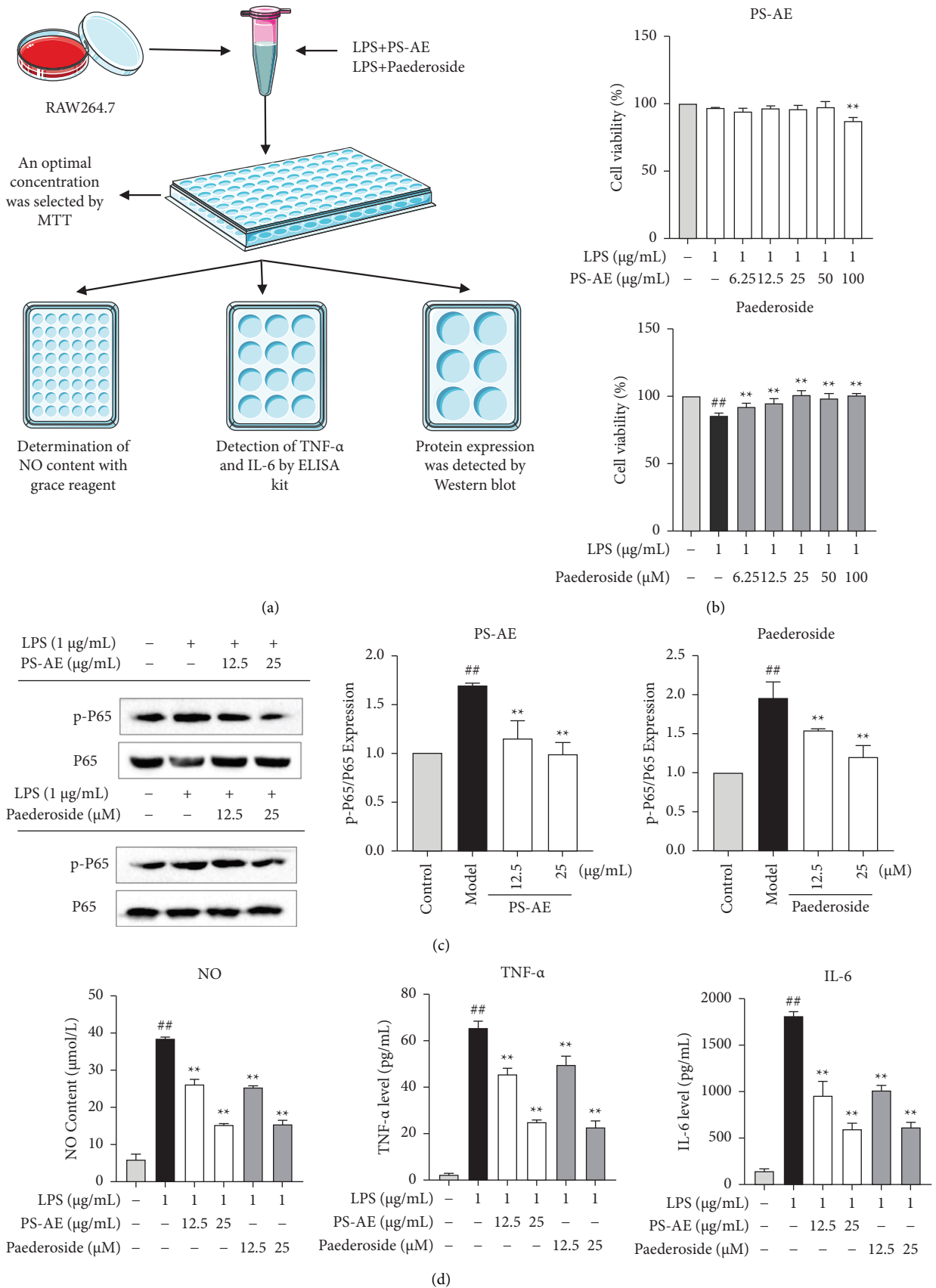


FIGURE 5: PS-AE and paederoside could significantly inhibit the activation of NF- $\kappa$ B p65 and the production of inflammatory factors in downstream cells in LPS-stimulated RAW264.7 cells: (a) the process for the *in vitro* study, (b) the cell viability was assessed by MTT assay, (c) the expression of NF- $\kappa$ B p65 in LPS-stimulated RAW264.7 cells ( $n = 3$ ), and (d) PS-AE, paederoside significantly inhibited productions of pro-inflammatory mediators in LPS-stimulated RAW264.7 cells. NO production was measured using Griess assay, and levels of cytokines including TNF- $\alpha$  and IL-6 were analysed using ELISA kits ( $n = 6$ ). Results are expressed as the mean  $\pm$  SD, \*\*  $p < 0.01$  vs. model group, and ##  $p < 0.01$  vs. control group.

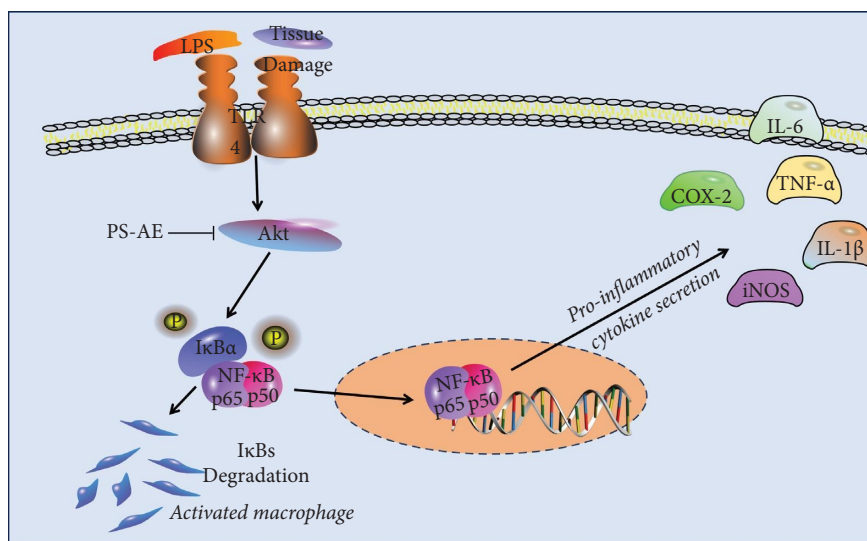


FIGURE 6: *Paederia scandens* (Lour.) Merr. protected gastric ulcer by regulating NF- $\kappa$ B signaling pathway.

promote the secretions of IL-1 $\beta$ , IL-6, and other cytokines, triggering a series of downstream inflammatory response [56, 57]. The results showed that PS-AE and paederoside significantly inhibited the LPS-induced activation of NF- $\kappa$ B p65 in RAW264.7 cells and suppressed the production of downstream cytokines NO, TNF- $\alpha$ , and IL-6.

Our findings demonstrated the protective effect of PS-AE on HCl/EtOH-induced gastric ulcer in rats and provide experimental evidence of *P. scandens* against gastric ulcer. Gastric ulcer in animals induced by diverse reagents/means including stress, pylorus ligation, acetic acid, and indomethacin have been widely reported and used to investigate the efficacy of potential agents [58]. The HCl/EtOH-induced gastric ulcer is commonly used and considered as a reliable model for studying the pathogenesis of gastritis and gastric ulcers, for its superiority in rapid induction of ulcer which greatly resembles gastric mucosal damage in human beings [59]. Although inconsistent with therapeutic treatment as common human-used drugs, prophylactic treatment, and dosing arrangement are widely accepted in recent experimental studies for primary efficacy evaluation [60, 61]. In our further study, a therapeutic treatment in model animals is warranted to evaluate the pharmacodynamic characteristics of PS-AE. In addition, we investigated the involvement of NF- $\kappa$ B signaling in the protective effect of PS-AE on gastric ulcer *in vitro* and *in vivo*. To further elucidate the mechanism of action of PS-AE against gastric ulcer, bioactive fraction/ingredient and crucial target/pathway of the PS-AE will be studied by using chemical analyses and biological technologies such as RNA-sequencing and knock-out animals.

## 5. Conclusion

The findings of this study demonstrated that the aqueous extract of the herb of *Paederia scandens* exerts a protective effect on HCl/EtOH-induced gastric ulcer in rats, which is probably associated with inhibition of the activities of

oxidative stress and pro-inflammatory mediators regulated by NF- $\kappa$ B signaling pathway (Figure 6). In addition, 13 potential NF- $\kappa$ B-targeting inhibitors are probably effective substances contributing to the herb's pharmacological effect. It provides pharmacological justifications for the functional food use of *Paederia scandens* for treating gastric diseases.

## Data Availability

The data used to support the findings of this study are available from the corresponding authors upon reasonable request.

## Conflicts of Interest

The authors declare that they have no conflicts of interest associated with the manuscript.

## Authors' Contributions

The published version of this work has been reviewed and approved by all authors. Qingxia Li and Hui Guo conducted experimental research and wrote the manuscript. Man Gong, Yang Zhang, and Lianhe Yang collected and analysed the data. Jing Wang and Pei Wang conducted the manuscript revision. Zhimin Wang, Erping Xu, and Liping Dai designed and supervised the study. Qingxia Li and Hui Guo contributed equally to this work.

## Acknowledgments

The present work was financially supported by the National Key Research and Development Program of China (no. 2017YFC1701904), the Key Research Project on Traditional Chinese Culture and Management of Henan (no. TCM2021013), The Cuiyingmin National Famous Old Chinese Medicine Expert Inheritance Studio Construction Project (no. 2022-75), Molecular Mechanism and Spectrum-Effect Relationship of Xingzhongheji Intervention in

Precancerous Lesions of Chronic Atrophic Gastritis (no. 222301420023), and Zhongjing Prescription for Chronic Atrophic Gastritis (no. 23IRTSTHN028).

## Supplementary Materials

Figure S1: UPLC chromatograms of PS-AE and the 6 components in mixed reference solution (the numbers in the figure indicate the number of chromatographic peaks: (1) paederoside acid, (2) rutin, (3) paederoside, (4) quercetin, (5) linarin, and (6) kaempferol). Figure S2: PS-AE dose dependently decreased the ulcer area in model rats. Table S1: the structures of both training and test set compounds. (*Supplementary Materials*)

## References

- [1] Y. Mai, S. Xu, R. Shen, B. Feng, H. He, and Y. Xu, "Gastroprotective effects of water extract of domesticated *Amauroderma rugosum* against several gastric ulcer models in rats," *Pharmaceutical Biology*, vol. 60, no. 1, pp. 600–608, 2022.
- [2] Y. S. Xia, Z. M. Li, C. Liu et al., "Preparation of deer oil powder and its effect on acute gastric mucosal injury in rats," *Journal of Food Biochemistry*, vol. 46, no. 5, Article ID e14088, 2022.
- [3] R. Liu, Y. T. Hao, N. Zhu et al., "The gastroprotective effect of small molecule oligopeptides isolated from walnut (*Juglans regia* L.) against ethanol-induced gastric mucosal injury in rats," *Nutrients*, vol. 12, no. 4, p. 1138, 2020.
- [4] B. B. da Luz, D. Maria-Ferreira, J. L. Dallazen et al., "Effectiveness of the polyphenols-rich *Sedum dendroideum* infusion on gastric ulcer healing in rats: roles of protective endogenous factors and antioxidant and anti-inflammatory mechanisms," *Journal of Ethnopharmacology*, vol. 278, Article ID 114260, 2021.
- [5] A. Giatromanolaki, A. Tsolou, E. Daridou, M. Kouroupi, K. Chlichlia, and M. I. Koukourakis, "iNOS expression by tumor-infiltrating lymphocytes, PD-L1 and prognosis in non-small-cell lung cancer," *Cancers*, vol. 12, no. 11, p. 3276, 2020.
- [6] R. Abo-Elsoud, S. Ahmed Mohamed Abdelaziz, M. Attia Abd Eldaim, and S. M. Hazzaa, "Moringa oleifera alcoholic extract protected stomach from bisphenol A-induced gastric ulcer in rats via its anti-oxidant and anti-inflammatory activities," *Environmental Science and Pollution Research*, vol. 29, no. 45, pp. 68830–68841, 2022.
- [7] M. R. Akanda, I. S. Kim, D. Ahn et al., "Anti-inflammatory and gastroprotective roles of *Rabdosia inflexa* through downregulation of pro-inflammatory cytokines and MAPK/NF- $\kappa$ B signaling pathways," *International Journal of Molecular Sciences*, vol. 19, no. 2, p. 584, 2018.
- [8] R. S. Aziz, A. Siddiqua, M. Shahzad, A. Shabbir, and N. Naseem, "Oxyresveratrol ameliorates ethanol-induced gastric ulcer via downregulation of IL-6, TNF- $\alpha$ , NF- $\kappa$ B, and COX-2 levels, and upregulation of TFF-2 levels," *Bio-medicine & Pharmacotherapy*, vol. 110, pp. 554–560, 2019.
- [9] W. S. Li, S. C. Lin, C. H. Chu et al., "The gastroprotective effect of naringenin against ethanol-induced gastric ulcers in mice through inhibiting oxidative and inflammatory responses," *International Journal of Molecular Sciences*, vol. 22, no. 21, p. 11985, 2021.
- [10] N. Ma, Y. Sun, J. Yi, L. Zhou, and S. Cai, "Chinese sumac (*Rhus chinensis* Mill.) fruits alleviate indomethacin-induced gastric ulcer in mice by improving oxidative stress, inflammation and apoptosis," *Journal of Ethnopharmacology*, vol. 284, Article ID 114752, 2022.
- [11] H. Song, X. Hou, M. Zeng et al., "Traditional Chinese Medicine Li-Zhong-Tang accelerates the healing of indomethacin-induced gastric ulcers in rats by affecting TLR-2/MyD88 signaling pathway," *Journal of Ethnopharmacology*, vol. 259, Article ID 112979, 2020.
- [12] C. P. Commission, *Pharmacopoeia of the People's Republic of China*, Chemical Industry Press, Beijing, China, 1977.
- [13] W. Jiang, D. Jin, Z. Li et al., "Characterization of multiple absorbed constituents in rats after oral administration of *Paederia scandens* decoction," *Biomedical Chromatography*, vol. 26, no. 7, pp. 863–868, 2012.
- [14] Y. Liu, W. Zhe, R. Zhang et al., "Ultrasonic-assisted extraction of polyphenolic compounds from *Paederia scandens* (Lour.) Merr. Using deep eutectic solvent: optimization, identification, and comparison with traditional methods," *Ultrasonics Sonochemistry*, vol. 86, Article ID 106005, 2022.
- [15] L. Wang, Y. Jiang, T. Han, C. Zheng, and L. Qin, "A phytochemical, pharmacological and clinical profile of *Paederia foetida* and *P. scandens*," *Natural Product Communications*, vol. 9, no. 6, Article ID 1934578X1400900, 2014.
- [16] Q. Wu, H. Tang, and H. Wang, "The anti-oxidation and mechanism of essential oil of *Paederia scandens* in the NAFLD model of chicken," *Animals*, vol. 9, no. 10, p. 850, 2019.
- [17] B. C. Chen, H. Y. He, K. Niu et al., "Network pharmacology-based approach uncovers the JAK/STAT signaling mechanism underlying *paederia scandens* extract treatment of rheumatoid arthritis," *Am J Transl Res*, vol. 14, no. 8, pp. 5295–5307, 2022.
- [18] M. Xiao, X. Fu, Y. Ni et al., "Protective effects of *Paederia scandens* extract on rheumatoid arthritis mouse model by modulating gut microbiota," *Journal of Ethnopharmacology*, vol. 226, pp. 97–104, 2018.
- [19] P. Wang, J. Chi, H. Guo et al., "Identification of differential compositions of aqueous extracts of *cinnamomi ramulus* and *cinnamomi cortex*," *Molecules*, vol. 28, no. 5, Article ID 28052015, 2023.
- [20] M. J. Hossen, J. Y. Chou, S. M. Li et al., "An ethanol extract of the rhizome of *Atractylodes chinensis* exerts anti-gastritis activities and inhibits Akt/NF- $\kappa$ B signaling," *Journal of Ethnopharmacology*, vol. 228, pp. 18–25, 2019.
- [21] Y. Faridvand, N. Bagherpour-Hassanlouei, S. Nozari et al., "1, 25-Dihydroxyvitamin D3 activates Apelin/APJ system and inhibits the production of adhesion molecules and inflammatory mediators in LPS-activated RAW264.7 cells," *Pharmacological Reports*, vol. 71, no. 5, pp. 811–817, 2019.
- [22] E. Gugliandolo, M. Cordaro, R. Fusco et al., "Protective effect of snail secretion filtrate against ethanol-induced gastric ulcer in mice," *Scientific Reports*, vol. 11, no. 1, p. 3638, 2021.
- [23] I. F. da Silva Junior, S. O. Balogun, R. G. de Oliveira, A. S. Damazo, and D. T. D. O. Martins, "Piper umbellatum L.: a medicinal plant with gastric-ulcer protective and ulcer healing effects in experimental rodent models," *Journal of Ethnopharmacology*, vol. 192, pp. 123–131, 2016.
- [24] H. Sahin, K. Kaltalioglu, Z. Erisgin, S. Coskun-Cevher, and S. Kolayli, "Protective effects of aqueous extracts of some honeys against HCl/ethanol-induced gastric ulceration in rats," *Journal of Food Biochemistry*, vol. 43, no. 12, Article ID e13054, 2019.
- [25] S. Byeon, J. Oh, J. S. Lim, J. S. Lee, and J. S. Kim, "Protective effects of *Dioscorea batatas* flesh and peel extracts against

- ethanol-induced gastric ulcer in mice," *Nutrients*, vol. 10, no. 11, p. 1680, 2018.
- [26] A. M. Ghanim, S. Rezaq, T. S. Ibrahim, D. G. Romero, and H. Kothayer, "Novel 1,2,4-triazine-quinoline hybrids: the privileged scaffolds as potent multi-target inhibitors of LPS-induced inflammatory response via dual COX-2 and 15-LOX inhibition," *European Journal of Medicinal Chemistry*, vol. 219, Article ID 113457, 2021.
- [27] H. Zeng, M. He, M. Yang, Z. Meng, H. Wang, and C. Wang, "In vitro and in vivo investigation on the effectiveness of alginate-based gastric mucosal protective gel," *BioMed Research International*, vol. 2022, Article ID 8287163, 11 pages, 2022.
- [28] Y. Wang, Y. Kang, C. Qi et al., "Pentoxifylline enhances antioxidative capability and promotes mitochondrial biogenesis for improving age-related behavioral deficits," *Aging (Albany NY)*, vol. 12, no. 24, pp. 25487–25504, 2020.
- [29] M. Gong, Q. Li, H. Guo et al., "Protective effect of active components of *Eucommia ulmoides* leaves on gastric ulcers in rats: involvement of the PI3K/Akt/NF- $\kappa$ B pathway," *Journal of Food Science*, vol. 87, no. 7, pp. 3207–3222, 2022.
- [30] J. M. Lim, C. H. Song, S. J. Park et al., "Protective effects of a triple-fermented barley extract (FBe) against HCl/EtOH-induced gastric mucosa damage in mice," *Food Sciences and Nutrition*, vol. 6, no. 8, pp. 2036–2046, 2018.
- [31] B. Whittle, "Gastrointestinal effects of nonsteroidal anti-inflammatory drugs," *Fundamental & Clinical Pharmacology*, vol. 17, no. 3, pp. 301–313, 2003.
- [32] R. M. Aman, R. A. Zaghoul, and M. S. El-Dahhan, "Formulation, optimization and characterization of allantoin-loaded chitosan nanoparticles to alleviate ethanol-induced gastric ulcer: in-vitro and in-vivo studies," *Scientific Reports*, vol. 11, no. 1, p. 2216, 2021.
- [33] M. Xie, H. Chen, S. Nie, W. Tong, J. Yin, and M. Xie, "Gastroprotective effect of gamma-aminobutyric acid against ethanol-induced gastric mucosal injury," *Chemico-Biological Interactions*, vol. 272, pp. 125–134, 2017.
- [34] F. L. Wang, Y. B. Ji, and B. Yang, "Sulfated modification, characterization and monosaccharide composition analysis of *Undaria pinnatifida* polysaccharides and anti-tumor activity," *Experimental and Therapeutic Medicine*, vol. 20, no. 1, pp. 630–636, 2020.
- [35] M. Alisik, T. Alisik, B. Nacir et al., "Erythrocyte reduced/oxidized glutathione and serum thiol/disulfide homeostasis in patients with rheumatoid arthritis," *Clinical Biochemistry*, vol. 94, pp. 56–61, 2021.
- [36] D. J. Balan, T. Rajavel, M. Das, S. Sathya, M. Jeyakumar, and K. P. Devi, "Thymol induces mitochondrial pathway-mediated apoptosis via ROS generation, macromolecular damage and SOD diminution in A549 cells," *Pharmacological Reports*, vol. 73, no. 1, pp. 240–254, 2021.
- [37] D. Shi, J. Zhou, L. Zhao et al., "Alleviation of mycotoxin biodegradation agent on zearalenone and deoxynivalenol toxicosis in immature gilts," *Journal of Animal Science and Biotechnology*, vol. 9, no. 1, p. 42, 2018.
- [38] D. D. Ilchovska and D. M. Barrow, "An Overview of the NF- $\kappa$ B mechanism of pathophysiology in rheumatoid arthritis, investigation of the NF- $\kappa$ B ligand RANKL and related nutritional interventions," *Autoimmunity Reviews*, vol. 20, no. 2, Article ID 102741, 2021.
- [39] X. Liu, S. Quan, Q. Han et al., "Effectiveness of the fruit of *Rosa odorata* sweet var. *gigantea* (Coll. et Hemsl.) Rehd. et Wils in the protection and the healing of ethanol-induced rat gastric mucosa ulcer based on Nrf2/NF- $\kappa$ B pathway regulation," *Journal of Ethnopharmacology*, vol. 282, Article ID 114626, 2022.
- [40] R. Maity, P. Mondal, M. K. Giri, C. Ghosh, and C. Mallick, "Gastroprotective effect of hydromethanolic extract of *Ayapana triplinervis* leaves on indomethacin-induced gastric ulcer in male Wistar rats," *Journal of Food Biochemistry*, vol. 45, no. 8, Article ID e13859, 2021.
- [41] A. Tanyeli, E. Eraslan, E. Polat, and T. Bal, "Protective effect of salusin- $\alpha$  and salusin- $\beta$  against ethanol-induced gastric ulcer in rats," *Journal of Basic and Clinical Physiology and Pharmacology*, vol. 28, no. 6, pp. 623–630, 2017.
- [42] Y. Liu, J. Liang, J. Wu et al., "Transformation of patchouli alcohol to  $\beta$ -patchoulene by gastric juice:  $\beta$ -patchoulene is more effective in preventing ethanol-induced gastric injury," *Scientific Reports*, vol. 7, no. 1, p. 5591, 2017.
- [43] J. Z. Wu, Y. H. Liu, J. L. Liang et al., "Protective role of  $\beta$ -patchoulene from *Pogostemon cablin* against indomethacin-induced gastric ulcer in rats: involvement of anti-inflammation and angiogenesis," *Phytomedicine*, vol. 39, pp. 111–118, 2018.
- [44] Y. Fu, Y. N. Sun, K. H. Yi et al., "3D pharmacophore-based virtual screening and docking approaches toward the Discovery of novel HPPD inhibitors," *Molecules*, vol. 22, no. 6, p. 959, 2017.
- [45] G. Luo, F. Lu, L. Qiao, X. Chen, G. Li, and Y. Zhang, "Discovery of potential inhibitors of aldosterone Synthase from Chinese herbs using pharmacophore modeling, molecular docking, and molecular dynamics simulation studies," *BioMed Research International*, vol. 2016, Article ID 4182595, 8 pages, 2016.
- [46] H. Hu, J. Xia, D. Wang, X. S. Wang, and S. Wu, "A thoroughly validated virtual screening strategy for Discovery of novel HDAC3 inhibitors," *International Journal of Molecular Sciences*, vol. 18, no. 1, p. 137, 2017.
- [47] Y. L. Wang, J. J. Yang, S. C. Dai et al., "Formation of soybean protein isolate-hawthorn flavonoids non-covalent complexes: linking the physicochemical properties and emulsifying properties," *Ultrasonics Sonochemistry*, vol. 84, Article ID 105961, 2022.
- [48] M. Gupta, M. Gulati, B. Kapoor et al., "Anti-ulcerogenic effect of methanolic extract of *Elaeagnus conferta* Roxb. seeds in Wistar rats," *Journal of Ethnopharmacology*, vol. 275, Article ID 114115, 2021.
- [49] O. J. Olatunji, H. Chen, and Y. Zhou, "Anti-Ulcerogenic properties of *Lycium chinense* mill extracts against ethanol-induced acute gastric lesion in animal models and its active constituents," *Molecules*, vol. 20, no. 2, pp. 22553–22564, 2015.
- [50] M. S. Abdelfattah, M. I. Y. Elmallah, H. Y. Ebrahim, R. S. Almeer, R. M. A. Eltanany, and A. E. Abdel Moneim, "Prodigiosins from a marine sponge-associated actinomycete attenuate HCl/ethanol-induced gastric lesion via antioxidant and anti-inflammatory mechanisms," *PLoS One*, vol. 14, no. 6, Article ID e0216737, 2019.
- [51] J. Li, Y. M. Xue, B. Zhu et al., "Rosiglitazone elicits an adiponectin-mediated insulin-sensitizing action at the adipose tissue-liver Axis in otsuka long-evans tokushima fatty rats," *Journal of Diabetes Research*, vol. 2018, Article ID 4627842, 12 pages, 2018.
- [52] N. N. H. Nik Salleh, F. A. Othman, N. A. Kamarudin, and S. C. Tan, "The biological activities and therapeutic potentials of baicalein extracted from *oroxyllum indicum*: a systematic review," *Molecules*, vol. 25, no. 23, p. 5677, 2020.

- [53] W. Peng, X. Q. Qiu, Z. H. Shu et al., "Hepatoprotective activity of total iridoid glycosides isolated from *Paederia scandens* (Lour.) Merr. var. *tomentosa*," *Journal of Ethnopharmacology*, vol. 174, pp. 317–321, 2015.
- [54] C. Park, H. J. Cha, H. Lee, G. Y. Kim, and Y. H. Choi, "The regulation of the TLR4/NF- $\kappa$ B and Nrf2/HO-1 signaling pathways is involved in the inhibition of lipopolysaccharide-induced inflammation and oxidative reactions by morroniside in RAW 264.7 macrophages," *Archives of Biochemistry and Biophysics*, vol. 706, Article ID 108926, 2021.
- [55] H. L. Hsieh, M. C. Yu, L. C. Cheng et al., "Quercetin exerts anti-inflammatory effects via inhibiting tumor necrosis factor- $\alpha$ -induced matrix metalloproteinase-9 expression in normal human gastric epithelial cells," *World Journal of Gastroenterology*, vol. 28, no. 11, pp. 1139–1158, 2022.
- [56] J. Hu, J. Luo, M. Zhang et al., "Protective effects of radix *sophorae flavescentis carbonisata*-based carbon dots against ethanol-induced acute gastric ulcer in rats: anti-inflammatory and antioxidant activities," *International Journal of Nanomedicine*, vol. 16, pp. 2461–2475, 2021.
- [57] Q. B. Zhang, D. Zhu, F. Dai et al., "MicroRNA-223 suppresses IL-1 $\beta$  and TNF- $\alpha$  production in gouty inflammation by targeting the NLRP3 inflammasome," *Frontiers in Pharmacology*, vol. 12, Article ID 637415, 2021.
- [58] M. Kapitonova, S. Gupalo, R. Alyautdin et al., "Gastroprotective effect of *Berberis vulgaris* on ethanol-induced gastric mucosal injury: histopathological evaluations," *Avicenna Journal Phytomed*, vol. 12, no. 1, pp. 30–41, 2022.
- [59] N. Abu Bakar, M. N. Hakim Abdullah, V. Lim, and Y. K. Yong, "Gastroprotective effect of polypeptide-K isolated from *Momordica charantia*'s seeds on multiple experimental gastric ulcer models in rats," *Evidence-based Complementary and Alternative Medicine*, vol. 2022, Article ID 6098929, 11 pages, 2022.
- [60] J. L. R. Martins, D. M. Silva, E. H. Gomes et al., "Evaluation of gastroprotective activity of linoleic acid on gastric ulcer in a mice model," *Current Pharmaceutical Design*, vol. 28, no. 8, pp. 655–660, 2022.
- [61] A. M. Mousa, N. M. El-Sammad, S. K. Hassan et al., "Anti-ulcerogenic effect of *Cuphea ignea* extract against ethanol-induced gastric ulcer in rats," *BMC Complementary and Alternative Medicine*, vol. 19, no. 1, p. 345, 2019.